

THE UNIVERSITY OF ADELAIDE

School of Electrical and Electronic Engineering

**On-line Condition Monitoring and
Detection of Stator and Rotor Faults in
Induction Motors**

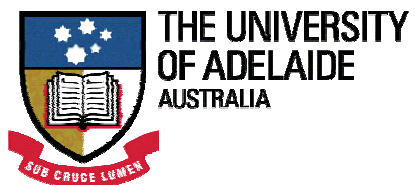
Randy Supangat

A thesis presented for the degree of Doctor of Philosophy

2008

Dedicated to my wife

© 2008
Randy Supangat
All Rights Reserved



On-line Condition Monitoring and Detection of Stator and Rotor Faults in Induction Motors

Randy Supangat

Submitted for the degree of Doctor of Philosophy

2008

Abstract

Induction motors are reliable and widely used in industrialised nations. However induction motors, like any other machine, will eventually fail. If the failure is not anticipated, it can result in a significant revenue loss. Therefore, there is a strong need to develop an efficient maintenance program. The most cost-effective solution is condition-based maintenance. An effective condition-based maintenance program requires an on-line condition monitoring system that can diagnose the condition of an induction motor in order to determine the types of faults and their severity while the motor is under a normal operating condition.

The work in this thesis investigates the detection of stator and rotor faults (i.e. shorted turn faults, eccentricity faults, and broken rotor bar faults) using three types of sensor signals (i.e. current, leakage flux, and vibration) under different loading conditions. The work is based on an extensive series of sensor measurements taken using a number of nominally identical healthy machines (2.2 kW) and custom-modified machines (2.2 kW) with configurable stator and rotor fault settings.

The thesis starts by investigating the estimation of rotor speed and rotor slot number. These two parameters are important in determining the fault frequency components that are used for detecting the stator and rotor faults. The rotor speed investigation compares four different estimation methods from the three different sensor signal types. It is found that the speed estimation techniques based on the eccentricity harmonics and the rotor frequency in the stator current, the axial leakage flux, and the motor vibration sensor signals can detect the rotor speed very accurately even when the load is as low as 2%. Similarly, this thesis proposes three different rotor slot number estimation techniques from the three different types of sensors and demonstrates that all three techniques can estimate the rotor slot number accurately. In addition, it is shown that the reliability of the estimation techniques can be increased significantly when the three techniques are combined.

The shorted turn investigation in this thesis examines and compares potential shorted turn features in the three sensor signal types under five different fault severities and ten different loading conditions. The useful shorted turn features are identified in the thesis, and then examined against variations between the healthy machines in order to determine the loads and the fault severities in which the feature can reliably detect the faults. The results show that the feature based on the EPVA (extended Park's vector approach) is the best method. This feature can detect turn to turn faults with a severity of 3.5% or greater at loads greater than 20% and phase to phase turn faults with a severity of 1.7% or greater under all loading conditions. However, estimating the fault severity is generally found to be difficult.

The thesis also examines the feasibility of detecting static eccentricity faults using the different types of sensor signals under ten different loading conditions. The thesis compares potential eccentricity features under nine different fault severities. The useful features are identified and then combined through weighted linear combination (WLC) in order to produce a better eccentricity fault indicator. The indicator begins to show significant magnitude variation when the fault severity is greater than or equal to 25% and the load is greater than or equal to 25%. The experimental results show that detecting the static eccentricity faults is possible but estimating the fault severity may be difficult. Furthermore, the effects of misalignment faults on the useful eccentricity features are investigated.

In this thesis, the analysis of broken rotor bar faults is performed under motor starting and rundown operation. The starting analysis introduces a new approach to detect broken rotor bar faults that utilises the wavelet transform of the envelope of the starting current waveform. The results of the wavelet transform are then processed in order to develop a normalised parameter, called the wavelet indicator. It is found that the wavelet indicator can detect a single broken bar under all loading conditions during motor starting operation. The indicator also increases its magnitude as the severity of the fault increases. On the other hand, the rundown analysis proposes several broken rotor bar fault detection techniques which utilise the induced voltage in the stator windings and the stator magnetic flux linkage after supply disconnection. The experimental results show that detecting the faults during rundown is generally difficult. However, the wavelet approach, which is based on monitoring changes in the motor torque for a given slip, seems to give the best result.

Declaration and Publications

This work contains no material which has been accepted for the award of any other degree or diploma in any university or other tertiary institution and, to the best of my knowledge and belief, contains no material previously published or written by another person, except where due reference has been made in the text.

I give consent to this copy of my thesis when deposited in the University Library, being made available for loan and photocopying, subject to the provisions of the Copyright Act 1968.

The author acknowledges that copyright of published works contained within this thesis (as listed below) resides with the copyright holder(s) of those works.

List of Publications

- [P1] I. Ahmed, R. Supangat, J. Grieger, N. Ertugrul, and W. L. Soong, "A Baseline Study for On-Line Condition Monitoring of Induction Machines," in Australasian Universities Power Engineering Conference (AUPEC), Brisbane, Australia, 2004.
- [P2] J. Grieger, R. Supangat, N. Ertugrul, and W. L. Soong, "Induction Motor Static Eccentricity Severity Estimation Using Evidence Theory," in IEEE International Electric Machines & Drives Conference (IEMDC), Antalya, Turkey, 2007, pp. 190-195.

- [P3] J. Grieger, R. Supangat, N. Ertugrul, W. L. Soong, D. A. Gray, and C. Hansen, "Estimation of Static Eccentricity Severity in Induction Motors for On-Line Condition Monitoring," in 41st IAS Annual Meeting Conference Record of the IEEE Industry Applications Conference (IAS), Tampa, FL, 2006, pp. 2312 - 2319.
- [P4] R. Supangat, N. Ertugrul, W. L. Soong, D. A. Gray, C. Hansen, and J. Grieger, "Broken Rotor Bar Fault Detection in Induction Motors Using Starting Current Analysis," in European Conference on Power Electronics and Applications, 2005.
- [P5] R. Supangat, N. Ertugrul, W. L. Soong, D. A. Gray, C. Hansen, and J. Grieger, "Detection of Broken Rotor Bars in Induction Motor Using Starting-Current Analysis and Effects of Loading," IEE Proceedings - Electric Power Applications, vol. 153, pp. 848 - 855, November 2006.
- [P6] R. Supangat, N. Ertugrul, W. L. Soong, D. A. Gray, C. Hansen, and J. Grieger, "Estimation of the Number of Rotor Slots and Rotor Speed in Induction Motors Using Current, Flux, or Vibration Signature Analysis," in Australasian Universities Power Engineering Conference (AUPEC) Melbourne, Australia: Victoria University, 2006.
- [P7] R. Supangat, J. Grieger, N. Ertugrul, W. L. Soong, D. A. Gray, and C. Hansen, "Investigation of Static Eccentricity Fault Frequencies using Multiple Sensors in Induction Motors and Effects of Loading," in IECON - 32nd Annual Conference on IEEE Industrial Electronics, Paris, France, 2006, pp. 958 - 963.
- [P8] R. Supangat, J. Grieger, N. Ertugrul, W. L. Soong, D. A. Gray, and C. Hansen, "Detection of Broken Rotor Bar Faults and Effects of Loading in Induction Motors during Rundown," in IEEE International Electric Machines & Drives Conference (IEMDC), Antalya, Turkey, 2007, pp. 196 - 201.

Pending Publications

- [P*] R. Supangat, N. Ertugrul, W. L. Soong, D. A. Gray, C. Hansen, and J. Grieger, "Estimation of the Number of Rotor Slots and Rotor Speed in Induction Motors Using Current, Flux, or Vibration Signature Analysis," Australian Journal of Electrical & Electronics Engineering (AJEEE).

Signed:

Date:

Acknowledgements

I would like to thank Assoc. Prof. Nesimi Ertugrul for his visions and guidance in directing the research. His supervision has been tremendous for the development of the project. I am also very grateful to Dr. Wen L. Soong for the insightful conversations, the advices, and the resources that he provided throughout the research. I also like to thank Prof. Colin Hansen and Prof. Douglas A. Gray for their supervisions and their invaluable inputs in improving the overall project.

My thanks also go to Jason Grieger and all members of the School of Electrical and Electronic Engineering in the University of Adelaide for their significant helps and supports.

Last but not least, this project would not have been possible without the generous supports from National Instruments Inc. USA and the funds from the ARC Linkage Grant LP0453951 (Integrated On-Line Condition Monitoring and Failure Diagnosis in Induction Motors).

Contents

| | |
|--|--------------|
| ABSTRACT | I |
| DECLARATION AND PUBLICATIONS | IV |
| ACKNOWLEDGEMENTS | VI |
| CONTENTS | VII |
| LIST OF FIGURES | XII |
| SYMBOLS | XIX |
| ABBREVIATIONS | XXIII |
| CHAPTER 1. INTRODUCTION | 1 |
| 1.1. BACKGROUND ON INDUCTION MOTORS | 1 |
| 1.2. ON-LINE CONDITION MONITORING | 3 |
| 1.3. LITERATURE REVIEW OF MOTOR’S FAULTS | 4 |
| 1.3.1. <i>Broken Rotor Bar Faults</i> | 5 |
| 1.3.2. <i>Eccentricity Faults</i> | 6 |
| 1.3.3. <i>Stator Related Faults</i> | 7 |
| 1.3.4. <i>Bearing Faults</i> | 8 |
| 1.4. OBJECTIVES OF THE THESIS | 8 |
| 1.5. FEATURES OF THE EXPERIMENTAL SETUP USED IN THE THESIS | 11 |
| 1.5.1. <i>Simulation of Broken Rotor Bar Faults</i> | 15 |
| 1.5.2. <i>Simulation of Eccentricity Faults</i> | 15 |
| 1.5.3. <i>Simulation of Shorted Turn Faults</i> | 16 |
| 1.6. CONTRIBUTIONS OF THE THESIS | 18 |
| 1.7. ORGANISATION OF THE THESIS..... | 19 |

| | |
|---|-----------|
| CHAPTER 2. SIGNAL PROCESSING TECHNIQUES | 23 |
| 2.1. INTRODUCTION..... | 23 |
| 2.2. FOURIER TRANSFORM | 23 |
| 2.2.1. <i>Discrete Fourier Transform</i> | 24 |
| 2.2.2. <i>Fast Fourier Transform (FFT)</i> | 26 |
| 2.2.3. <i>Limitations of Practical Fourier Transform</i> | 26 |
| 2.2.3.1. Window Functions | 27 |
| 2.2.3.2. Interpolation in Frequency Domain..... | 31 |
| 2.2.3.3. Spectral Averaging..... | 32 |
| 2.3. SHORT-TIME FOURIER TRANSFORM..... | 35 |
| 2.3.1. <i>Short-Time Discrete Fourier Transform</i> | 36 |
| 2.4. WAVELET TRANSFORM | 37 |
| 2.4.1. <i>Continuous Wavelet Transform</i> | 40 |
| 2.4.2. <i>Discrete Wavelet Transform</i> | 41 |
| 2.5. ORDER TRACKING ANALYSIS..... | 43 |
| 2.6. SUMMARY | 43 |
| CHAPTER 3. ROTOR SPEED AND ROTOR SLOT NUMBER ESTIMATION | 45 |
| 3.1. INTRODUCTION..... | 45 |
| 3.2. ROTOR SPEED ESTIMATION TECHNIQUES..... | 47 |
| 3.2.1. <i>Stator Current</i> | 48 |
| 3.2.2. <i>Motor Vibration</i> | 48 |
| 3.2.3. <i>Axial Leakage Flux</i> | 49 |
| 3.2.4. <i>Comparison of Rotor Speed Estimation Techniques</i> | 50 |
| 3.3. ROTOR SLOT NUMBER ESTIMATION TECHNIQUES..... | 53 |
| 3.3.1. <i>Stator Current and Axial Leakage Flux</i> | 53 |
| 3.3.2. <i>Motor Vibration</i> | 57 |
| 3.3.3. <i>Comparison of Rotor Slot Number Estimation Techniques</i> | 60 |
| 3.3.4. <i>Combining Rotor Slot Number Estimation Techniques</i> | 62 |
| 3.4. SUMMARY | 64 |
| CHAPTER 4. BASELINE STUDY OF INDUCTION MOTORS..... | 67 |
| 4.1. INTRODUCTION..... | 67 |
| 4.2. APPROACH USED IN BASELINE STUDY | 68 |
| 4.3. FUNDAMENTAL FREQUENCY | 72 |
| 4.3.1. <i>Repeatability Test</i> | 72 |
| 4.3.2. <i>Motor Variation Test</i> | 73 |
| 4.4. BROKEN ROTOR BAR FAULT FREQUENCIES | 74 |
| 4.4.1. <i>Phase Variation Test</i> | 74 |
| 4.4.2. <i>Repeatability Test</i> | 75 |
| 4.4.3. <i>Motor Variation Test</i> | 76 |
| 4.5. ECCENTRICITY FAULT FREQUENCIES | 79 |
| 4.5.1. <i>Rotor slot harmonics</i> | 80 |
| 4.5.1.1. Phase Variation Test | 80 |
| 4.5.1.2. Repeatability Test..... | 80 |
| 4.5.1.3. Motor Variation Test..... | 81 |
| 4.5.2. <i>Rotor Frequency Sidebands of the Fundamental</i> | 84 |
| 4.5.2.1. Phase Variation Test | 84 |
| 4.5.2.2. Repeatability Test..... | 84 |
| 4.5.2.3. Motor Variation Test..... | 85 |
| 4.5.3. <i>Rotor Frequency</i> | 87 |

| | |
|---|------------|
| 4.5.3.1. Repeatability Test | 87 |
| 4.5.3.2. Motor Variation Test | 89 |
| 4.6. SHORTED TURN FAULT FREQUENCIES | 90 |
| 4.6.1. <i>Harmonics of Fundamental Sidebands of Rotor Frequency</i> | 91 |
| 4.6.1.1. Phase Variation Test | 91 |
| 4.6.1.2. Repeatability Test | 92 |
| 4.6.1.3. Motor Variation Test | 93 |
| 4.6.2. <i>Twice Supply Frequency</i> | 96 |
| 4.6.2.1. Repeatability Test | 96 |
| 4.6.2.2. Motor Variation Test | 98 |
| 4.7. SUMMARY | 99 |
| CHAPTER 5. SHORTED TURN FAULT DETECTION | 101 |
| 5.1. INTRODUCTION | 101 |
| 5.2. SHORTED TURN FAULT DETECTION TECHNIQUES | 103 |
| 5.2.1. <i>Fault Frequency Components in Current and Leakage Flux</i> | 105 |
| 5.2.2. <i>Fault Frequency Component in Vibration</i> | 105 |
| 5.2.3. <i>Extended Park's Vector Approach (EPVA)</i> | 106 |
| 5.3. ANALYSIS OF TURN TO TURN FAULTS | 108 |
| 5.3.1. <i>Using Fundamental Sidebands of Rotor Frequency Harmonics</i> | 108 |
| 5.3.2. <i>Using Twice Supply Frequency</i> | 113 |
| 5.3.3. <i>Using Rotor Slot Harmonics</i> | 114 |
| 5.3.4. <i>Using Third Harmonic of the Fundamental</i> | 116 |
| 5.3.5. <i>Using Extended Park's Vector Approach (EPVA)</i> | 117 |
| 5.3.6. <i>Summary of Effective Turn to Turn Features</i> | 119 |
| 5.3.6.1. Usability of the Ideal Turn to Turn Features | 121 |
| 5.4. ANALYSIS OF PHASE TO PHASE TURN FAULTS | 126 |
| 5.4.1. <i>Using Fundamental Sidebands of Rotor Frequency Harmonics</i> | 126 |
| 5.4.2. <i>Using Twice Supply Frequency</i> | 129 |
| 5.4.3. <i>Using Rotor Slot Harmonics</i> | 129 |
| 5.4.4. <i>Using Third Harmonic of the Fundamental</i> | 130 |
| 5.4.5. <i>Using Extended Park's Vector Approach (EPVA)</i> | 131 |
| 5.4.6. <i>Summary of Effective Phase to Phase Turn Features</i> | 132 |
| 5.4.6.1. Usability of the Ideal Phase to Phase Turn Features | 133 |
| 5.5. SUMMARY | 137 |
| CHAPTER 6. STATIC ECCENTRICITY FAULT DETECTION | 139 |
| 6.1. INTRODUCTION | 139 |
| 6.2. ECCENTRICITY FAULT DETECTION TECHNIQUES | 142 |
| 6.2.1. <i>Current and Flux Monitoring</i> | 143 |
| 6.2.2. <i>Vibration Monitoring</i> | 145 |
| 6.3. ANALYSIS OF STATIC ECCENTRICITY FAULTS | 145 |
| 6.3.1. <i>Using Rotor Slot Harmonics</i> | 146 |
| 6.3.1.1. Static Eccentricity Components | 146 |
| 6.3.1.2. Dynamic Eccentricity Components (Under Static Eccentricity Faults) | 150 |
| 6.3.2. <i>Using Rotor Frequency Sidebands of the Fundamental</i> | 151 |
| 6.3.3. <i>Using Rotor Frequency Sidebands of Twice the Fundamental</i> | 153 |
| 6.3.4. <i>Using Third Harmonic of Rotor Frequency</i> | 154 |
| 6.3.5. <i>Using Twice Supply Frequency</i> | 154 |
| 6.3.6. <i>Using Rotor Frequency</i> | 154 |
| 6.3.7. <i>Using Second Harmonic of Rotor Frequency Sidebands of the Fundamental</i> | 155 |
| 6.3.8. <i>Using RMS Vibration</i> | 155 |

| | |
|--|------------|
| 6.3.9. <i>Summary of Effective Static Eccentricity Features</i> | 156 |
| 6.4. COMBINING STATIC ECCENTRICITY FEATURES | 158 |
| 6.5. ANALYSIS OF MIXED STATIC ECCENTRICITY AND MISALIGNMENT FAULTS | 161 |
| 6.5.1. <i>Using Rotor Frequency</i> | 162 |
| 6.5.2. <i>Using Third Harmonic of Rotor Frequency</i> | 162 |
| 6.5.3. <i>Effects of Misalignment on Ideal Eccentricity Features</i> | 163 |
| 6.5.4. <i>Effects of Misalignment on Non-Concentric Eccentricity Features</i> | 164 |
| 6.5.5. <i>WLC of Eccentricity Features Under Mixed Faults</i> | 165 |
| 6.6. SUMMARY | 166 |
| CHAPTER 7. BROKEN ROTOR BAR FAULT DETECTION DURING STARTING | 169 |
| 7.1. INTRODUCTION | 169 |
| 7.2. CONTINUOUS WAVELET TRANSFORM OF STARTING CURRENT | 172 |
| 7.2.1. <i>Continuous Wavelet Transform of the Envelope of Starting Current</i> | 174 |
| 7.2.2. <i>Wavelet indicator</i> | 180 |
| 7.3. EXPERIMENTAL RESULTS AND ANALYSIS | 181 |
| 7.3.1. <i>Variability of Test Setup and Wavelet Technique</i> | 183 |
| 7.3.2. <i>Variability between Different Current Phases</i> | 185 |
| 7.3.3. <i>Comparison and Classification of Healthy and Faulty Motors</i> | 186 |
| 7.3.4. <i>Motors with Unbalanced Supply</i> | 187 |
| 7.4. SUMMARY | 189 |
| CHAPTER 8. BROKEN ROTOR BAR FAULT DETECTION DURING RUNDOWN | 191 |
| 8.1. INTRODUCTION | 191 |
| 8.2. DESCRIPTION OF BROKEN ROTOR BAR DETECTION TECHNIQUES DURING RUNDOWN | 193 |
| 8.3. ANALYSIS OF RUNDOWN BROKEN ROTOR BAR FEATURES USING INDUCED VOLTAGE | 196 |
| 8.3.1. <i>Harmonic Components</i> | 198 |
| 8.3.1.1. <i>Analysis of Results</i> | 199 |
| 8.3.2. <i>Rate of Decay of Rotor Speed for a Given Operating Slip</i> | 204 |
| 8.3.2.1. <i>Analysis of Results</i> | 205 |
| 8.4. ANALYSIS OF RUNDOWN BROKEN ROTOR BAR FEATURES USING STATOR FLUX LINKAGE | 208 |
| 8.4.1. <i>Step Change in Magnitude of Flux Linkage on Disconnection</i> | 211 |
| 8.4.1.1. <i>Analysis of Results</i> | 211 |
| 8.5. ANALYSIS OF RUNDOWN BROKEN ROTOR BAR FEATURES USING SPACE VECTOR OF STATOR FLUX LINKAGE | 212 |
| 8.5.1. <i>Time Constant of Stator Magnetic Flux Linkage</i> | 214 |
| 8.5.1.1. <i>Analysis of Results</i> | 215 |
| 8.5.2. <i>Harmonic Components</i> | 216 |
| 8.5.2.1. <i>Analysis of Results</i> | 217 |
| 8.6. SUMMARY | 222 |
| CHAPTER 9. THESIS SUMMARY AND RECOMMENDATION FOR FUTURE WORK | 225 |
| 9.1. INTRODUCTION | 225 |
| 9.2. SUMMARY OF WORK | 226 |
| 9.2.1. <i>Experimental Setup</i> | 226 |
| 9.2.2. <i>Rotor Speed Estimation</i> | 227 |
| 9.2.3. <i>Rotor Slot Number Estimation</i> | 227 |
| 9.2.4. <i>Baseline Study</i> | 228 |
| 9.2.5. <i>Shorted Turn Fault Detection</i> | 229 |
| 9.2.6. <i>Static Eccentricity Fault Detection</i> | 230 |
| 9.2.7. <i>Broken Rotor Bar Fault Detection</i> | 232 |

| | |
|--|------------|
| 9.3. FUTURE WORK..... | 235 |
| APPENDIX A. FURTHER DISCUSSION AND RESULTS OF THE SHORTED TURN FAULT TEST | 237 |
| A.1. CURRENT HARMONICS INDUCED IN THE ROTOR WINDING | 237 |
| A.2. CURRENT HARMONICS INDUCED IN THE STATOR WINDING..... | 239 |
| A.3. EXPERIMENTAL RESULTS FOR TURN TO TURN FAULT ANALYSIS USING FUNDAMENTAL SIDEBANDS OF ROTOR FREQUENCY HARMONICS..... | 240 |
| A.4. EXPERIMENTAL RESULTS FOR TURN TO TURN FAULT ANALYSIS USING TWICE SUPPLY FREQUENCY | 245 |
| A.5. EXPERIMENTAL RESULTS FOR TURN TO TURN FAULT ANALYSIS USING ROTOR SLOT HARMONICS .. | 246 |
| A.6. EXPERIMENTAL RESULTS FOR TURN TO TURN FAULT ANALYSIS USING THIRD HARMONIC OF THE FUNDAMENTAL | 252 |
| A.7. EXPERIMENTAL RESULTS FOR PHASE TO PHASE TURN FAULT ANALYSIS USING FUNDAMENTAL SIDEBANDS OF ROTOR FREQUENCY HARMONICS..... | 253 |
| A.8. EXPERIMENTAL RESULTS FOR PHASE TO PHASE TURN FAULT ANALYSIS USING TWICE SUPPLY FREQUENCY | 254 |
| A.9. EXPERIMENTAL RESULTS FOR PHASE TO PHASE TURN FAULT ANALYSIS USING ROTOR SLOT HARMONICS | 255 |
| A.10. EXPERIMENTAL RESULTS FOR PHASE TO PHASE TURN FAULT ANALYSIS USING THIRD HARMONIC OF THE FUNDAMENTAL | 256 |
| APPENDIX B. FURTHER RESULTS OF THE STATIC ECCENTRICITY FAULT TEST | 259 |
| B.1. EXPERIMENTAL RESULTS FOR STATIC ECCENTRICITY FAULT ANALYSIS USING ROTOR SLOT HARMONICS | 259 |
| B.2. EXPERIMENTAL RESULTS FOR STATIC ECCENTRICITY FAULT ANALYSIS USING ROTOR FREQUENCY SIDEBANDS OF THE FUNDAMENTAL | 261 |
| B.3. EXPERIMENTAL RESULTS FOR STATIC ECCENTRICITY FAULT ANALYSIS USING ROTOR FREQUENCY SIDEBANDS OF TWICE THE FUNDAMENTAL | 263 |
| B.4. EXPERIMENTAL RESULTS FOR STATIC ECCENTRICITY FAULT ANALYSIS USING THIRD HARMONIC OF ROTOR FREQUENCY | 264 |
| B.5. EXPERIMENTAL RESULTS FOR STATIC ECCENTRICITY FAULT ANALYSIS USING TWICE SUPPLY FREQUENCY | 265 |
| B.6. EXPERIMENTAL RESULTS FOR STATIC ECCENTRICITY FAULT ANALYSIS USING ROTOR FREQUENCY | 266 |
| B.7. EXPERIMENTAL RESULTS FOR STATIC ECCENTRICITY FAULT ANALYSIS USING SECOND HARMONIC OF ROTOR FREQUENCY SIDEBANDS OF THE FUNDAMENTAL | 266 |
| B.8. EXPERIMENTAL RESULTS FOR STATIC ECCENTRICITY FAULT ANALYSIS USING RMS VIBRATION | 267 |
| REFERENCE LIST..... | 269 |

List of Figures

| | |
|--|----|
| Figure 1.1 - Type of faults in induction motors. | 5 |
| Figure 1.2 – Example of a steady-state current waveform. | 11 |
| Figure 1.3 – Example of a starting current waveform. | 11 |
| Figure 1.4 – Example of a rundown induced voltage waveform. | 11 |
| Figure 1.5 - Photograph of the data acquisition and data analysis hardware (left) and the motor test setup (right). | 13 |
| Figure 1.6 - Block diagram of the measurement hardware and the motor test setup with the sensors' locations. | 14 |
| Figure 1.7 - Photograph of the rotor cross-section and the profile of the partially broken rotor bars. | 15 |
| Figure 1.8 - Sectioned view of the test motor showing the adjustable static eccentricity arrangement. | 16 |
| Figure 1.9 –Test motor showing the adjustable shorted turn arrangement. | 17 |
| Figure 1.10 – Illustration of the stator winding external accesses. | 17 |
| Figure 2.1 – Stator current signal of the healthy motor sampled at 8 kHz. | 29 |
| Figure 2.2 – Frequency spectrum of the stator current without any window function (or Rectangular window). | 30 |
| Figure 2.3 – Frequency spectrum of the stator current with Hanning window. | 30 |
| Figure 2.4 – Main peak (main lobe) of the fundamental component of the stator current with no zero padding (a), $3N$ zero padding (b), $7N$ zero padding (c), and $15N$ zero padding (d). | 32 |

| | |
|--|----|
| Figure 2.5 – Frequency spectrum of the stator current with no averaging. | 33 |
| Figure 2.6 – Frequency spectrum of the stator current with 5 blocks averaging..... | 34 |
| Figure 2.7 – Frequency spectrum of the stator current with 10 blocks averaging..... | 34 |
| Figure 2.8 – Illustration of the principle of STFT. | 36 |
| Figure 2.9 – Spectrogram of the stator current in Figure 2.1 with 20 blocks (top) and 100 blocks (bottom) division. | 37 |
| Figure 2.10 – Illustration of the principle of wavelet transform..... | 39 |
| Figure 2.11 – Examples of wavelet functions from the Daubechies family (db), the Coiflets family (coif), and the Symlet family (sym). | 39 |
| Figure 2.12 – Stator current signal of a healthy motor running at full load. | 41 |
| Figure 2.13 – CWT of the stator current signal. | 41 |
| Figure 2.14 – Multiple level wavelet decomposition. | 42 |
| Figure 3.1 - Frequency spectrum of the stator current signal at full load illustrating the eccentricity harmonics (Eq. 3.1). | 48 |
| Figure 3.2 - Frequency spectrum of the vibration signal at full load showing the rotor frequency. | 49 |
| Figure 3.3 - Frequency spectrum of the axial leakage flux signal at full load showing: (top) the eccentricity harmonics (Eq. 3.1), and (bottom) the slip frequency..... | 50 |
| Figure 3.4 - SNR of the rotor speed estimation techniques as a function of load. | 52 |
| Figure 3.5 - Frequency spectrum of the stator current signal showing the eccentricity harmonic based on (Eq. 3.7). | 54 |
| Figure 3.6 - Frequency spectrum of the axial leakage flux signal showing the eccentricity harmonic based on (Eq. 3.7). | 54 |
| Figure 3.7 - Magnitudes of the possible eccentricity component (Eq. 3.7) against the possible number of rotor slots in the stator current spectrum..... | 56 |
| Figure 3.8 - Magnitudes of the possible eccentricity component (Eq. 3.7) against the possible number of rotor slots in the axial flux spectrum..... | 56 |
| Figure 3.9 - Frequency spectrum of the motor vibration signal showing the rotor slot passing frequency (Eq. 3.8). | 58 |
| Figure 3.10 - Magnitudes of the possible rotor slot passing frequencies (Eq. 3.8) against the possible number of rotor slots in the vibration spectrum..... | 59 |
| Figure 3.11 - SNR of the rotor slot number estimation techniques for the healthy motor. . | 61 |
| Figure 3.12 - SNR of the rotor slot number estimation techniques for the faulty motor (4 BRB)..... | 61 |
| Figure 3.13 - Magnitudes of the combined rotor slot number estimation techniques using (Eq. 3.10) as a function of the possible number of rotor slots..... | 63 |
| Figure 3.14 - SNR of the combined rotor slot number estimation techniques for the healthy and faulty (4 BRB) motors..... | 64 |
| Figure 4.1 - Measured line voltage signal between phase A and B sampled at 400 Hz (top) and its corresponding frequency spectrum (bottom). | 70 |
| Figure 4.2 - Measured stator current signal of phase A sampled at 400 Hz (top) and its corresponding frequency spectrum (bottom)..... | 71 |

| | |
|---|----|
| Figure 4.3 - Measured axial leakage flux signal sampled at 400 Hz (top) and its corresponding frequency spectrum (bottom). | 71 |
| Figure 4.4 - Measured motor vibration signal at DEH sampled at 8 kHz (top) and its corresponding frequency spectrum (bottom). | 72 |
| Figure 4.5 - Repeatability test of the fundamental component. | 73 |
| Figure 4.6 - Motor variation test of the fundamental component. | 74 |
| Figure 4.7 – Phase variation test of the BRB sidebands. | 75 |
| Figure 4.8 – Repeatability test of the lower BRB sidebands. | 76 |
| Figure 4.9 – Repeatability test of the upper BRB sidebands. | 76 |
| Figure 4.10 – Example of the lower BRB sidebands in the current signals from the six identical motors. | 78 |
| Figure 4.11 – Motor variation test of the lower BRB sidebands. | 78 |
| Figure 4.12 – Motor variation test of the upper BRB sidebands. | 79 |
| Figure 4.13 – Phase variation test of the rotor slot harmonics. | 80 |
| Figure 4.14 – Repeatability test of the lower sideband of the fault frequencies in (Eq. 4.3). | 81 |
| Figure 4.15 - Repeatability test of the upper sideband of the fault frequencies in (Eq. 4.3). | 81 |
| Figure 4.16 – Motor variation test of the lower sideband of the fault frequencies in (Eq. 4.3). | 83 |
| Figure 4.17 - Motor variation test of the upper sideband of the fault frequencies in (Eq. 4.3). | 83 |
| Figure 4.18 – Phase variation test of the rotor frequency sidebands of the fundamental. ... | 84 |
| Figure 4.19 – Repeatability test of the lower sideband of the fault frequencies in (Eq. 1.3). | 85 |
| Figure 4.20 - Repeatability test of the upper sideband of the fault frequencies in (Eq. 1.3). | 85 |
| Figure 4.21 – Motor variation test of the lower sideband of the fault frequencies in (Eq. 1.3). | 86 |
| Figure 4.22 - Motor variation test of the upper sideband of the fault frequencies in (Eq. 1.3). | 87 |
| Figure 4.23 - Repeatability test of the fault frequencies in (Eq. 1.4) from the DEH vibration signal. | 88 |
| Figure 4.24 - Repeatability test of the fault frequencies in (Eq. 1.4) from the NDEH vibration signal. | 88 |
| Figure 4.25 - Repeatability test of the fault frequencies in (Eq. 1.4) from the DEV vibration signal. | 89 |
| Figure 4.26 – Motor variation test of the fault frequencies in (Eq. 1.4) from the three vibration signals. | 90 |
| Figure 4.27 – Phase variation test of the lower rotor frequency sideband harmonic. | 91 |
| Figure 4.28 - Phase variation test of the upper rotor frequency sideband harmonic. | 92 |

| | |
|--|-----|
| Figure 4.29 - Repeatability test of the lower sideband of the fault frequencies in (Eq. 4.4). | 93 |
| Figure 4.30 - Repeatability test of the upper sideband of the fault frequencies in (Eq. 4.4). | 93 |
| Figure 4.31 – Motor variation test of the lower sideband of the fault frequencies in (Eq. 4.4). | 95 |
| Figure 4.32 - Motor variation test of the upper sideband of the fault frequencies in (Eq. 4.4). | 95 |
| Figure 4.33 - Repeatability test of the fault frequencies in (Eq. 1.6) from the DEH vibration signal. | 96 |
| Figure 4.34 - Repeatability test of the fault frequencies in (Eq. 1.6) from the NDEH vibration signal. | 97 |
| Figure 4.35 - Repeatability test of the fault frequencies in (Eq. 1.6) from the DEV vibration signal. | 97 |
| Figure 4.36 – Motor variation test of the fault frequencies in (Eq. 1.6) from the three vibration signals. | 98 |
| Figure 5.1 – Park’s current vector representations of an ideal system (left) and a system with stator asymmetry (right). | 107 |
| Figure 5.2 – Magnitude of the frequency components in (Eq. 5.1) at $k = 1$, $\nu = -1$ (top), $k =$ 1 , $\nu = +1$ (bottom), from the current (left column) and leakage (right column) flux signals as a function of load. | 110 |
| Figure 5.3 – Typical Park’s vector locus of the three phase stator currents (top) and spectrum of the magnitude of the Park’s vector components (bottom). | 118 |
| Figure 5.4 – Magnitude of the EPVA feature as a function of load. | 118 |
| Figure 5.5 – Magnitude of the frequency components in (Eq. 5.1) at $k = 1$ and $\nu = -1$ in the leakage flux signal as a function of load. | 124 |
| Figure 5.6 – Magnitude of the frequency components in (Eq. 5.1) at $k = 1$ and $\nu = +1$ in the leakage flux signal as a function of load. | 124 |
| Figure 5.7 – Magnitude of the frequency components in (Eq. 5.1) at $k = 1$ and $\nu = -3$ in the leakage flux signal as a function of load. | 125 |
| Figure 5.8 – Magnitude of the frequency components in (Eq. 5.1) at $k = 1$ and $\nu = +3$ in the leakage flux signal as a function of load. | 125 |
| Figure 5.9 – Magnitude of the EPVA feature as a function of load. | 126 |
| Figure 5.10 – Magnitude of the frequency components in (Eq. 5.1) at $k = 1$, $\nu = \pm 1$ from the leakage flux signal as a function of load. | 127 |
| Figure 5.11 - Magnitude of the EPVA feature as a function of load. | 131 |
| Figure 5.12 – Magnitude of the frequency component in (Eq. 5.1) at $k = 1$ and $\nu = -1$ from the leakage flux signal as a function of load. | 134 |
| Figure 5.13 – Magnitude of the frequency component in (Eq. 5.1) at $k = 1$ and $\nu = +3$ from the leakage flux signal as a function of load. | 135 |
| Figure 5.14 – Magnitude of the frequency component in (Eq. 5.3) at $n_d = 0$, $k = 1$ and $\nu =$ $+1$ from the leakage flux signal as a function of load. | 136 |

| | |
|--|-----|
| Figure 5.15 – Magnitude of the EPVA feature as a function of load. | 137 |
| Figure 6.1 - Magnitude of the lower sideband of the static eccentricity components in (Eq. 6.1) from the current and the leakage flux signals as a function of load (top) and as a function of static eccentricity level (bottom). | 148 |
| Figure 6.2 – Magnitude of the upper sideband of the static eccentricity components in (Eq. 6.1) from the current and the leakage flux signals as a function of load (top) and as a function of static eccentricity level (bottom). | 149 |
| Figure 6.3 - WLC of the eccentricity features as a function of load (top) and as a function of static eccentricity level (bottom). | 160 |
| Figure 6.4 – Magnitude of the rotor frequency (Eq. 6.6) in the vibration signal under the mixed static eccentricity and misalignment faults: as a function of load (left) and as a function of static eccentricity level (right). | 162 |
| Figure 6.5 – Magnitude of the third harmonic of the rotor frequency (Eq. 6.4) in the vibration signal under the mixed static eccentricity and misalignment faults: as a function of load (left) and as a function of static eccentricity level (right). | 163 |
| Figure 6.6 – Magnitude of the ideal eccentricity features under the mixed (static eccentricity and misalignment) fault conditions. | 164 |
| Figure 6.7 – Magnitude of the non-concentric eccentricity features under the mixed (static eccentricity and misalignment) fault conditions. | 165 |
| Figure 6.8 - WLC of the eccentricity features as a function of static eccentricity level under the mixed (static eccentricity and misalignment) fault conditions. | 166 |
| Figure 7.1 - Starting current (phase A) signal (top) and continuous wavelet transform of the starting current signal (bottom) of the healthy motor. | 173 |
| Figure 7.2 - Starting current (phase A) signal (top) and continuous wavelet transform of the starting current signal (bottom) of the faulty motor with 4 BRB. | 174 |
| Figure 7.3 – Example of a transient signal and its components. | 176 |
| Figure 7.4 - Implementation flow diagram of the envelope extraction. | 177 |
| Figure 7.5 - Envelope of the starting current signal (top) and its continuous wavelet transform (bottom) of the healthy motor. | 179 |
| Figure 7.6 - Envelope of the starting current signal (top) and its continuous wavelet transform (bottom) of the faulty motor with 4 BRB. | 179 |
| Figure 7.7 - Wavelet indicator plot of the starting current under various loading conditions for the healthy motor and the faulty motor with 4 BRB. | 180 |
| Figure 7.8 - Starting current characteristics of the healthy motor running at no load. | 182 |
| Figure 7.9 - Starting current characteristics of the healthy motor running at full load. | 182 |
| Figure 7.10 - Starting current characteristics of the faulty motor (4 BRB) running at full load. | 183 |
| Figure 7.11 - Wavelet indicator plots for the starting current of three healthy motors and one faulty motor with 1 BRB as a function of load. | 184 |
| Figure 7.12 - Wavelet indicator plots for the starting current of a healthy motor with different initial rotor positions and supply voltage phase angles as a function of load. | 185 |

| | |
|--|-----|
| Figure 7.13 - Wavelet indicator plots for the starting current of the three different phases of the healthy motor. | 186 |
| Figure 7.14 - Wavelet indicator plots for the starting current of all tested motors..... | 187 |
| Figure 7.15 - Envelope of the starting current (top) and its continuous wavelet transform (bottom) for a motor with 33% of current unbalance. | 188 |
| Figure 7.16 - Wavelet indicator plots for the healthy motors and the motors with unbalanced supply..... | 189 |
| Figure 8.1 - Illustration of the measured components of the induced back-emf before and after supply disconnection. | 195 |
| Figure 8.2 - Rundown stator induced voltage on the healthy motor when operating at no-load (top) and full-load (bottom) before and after the supply disconnection (at 0 s). | 197 |
| Figure 8.3 - Rundown stator induced voltage on the faulty motor with 4 BRB when operating at no-load (top) and full-load (bottom) before and after the supply disconnection (at 0 s). | 197 |
| Figure 8.4 - Power spectra of the rundown induced voltages of the healthy motor running at no load (top) and at rated load (bottom). | 200 |
| Figure 8.5 - Power spectra of the rundown induced voltages of the faulty motor with 4 BRB running at no load (top) and at rated load (bottom). | 200 |
| Figure 8.6 - Power spectra (with OT technique) of the rundown induced voltages of the healthy motor running at no load (top) and at rated load (bottom). | 201 |
| Figure 8.7 - Power spectra (with OT technique) of the rundown induced voltages of the faulty motor with 4 BRB running at no load (top) and at rated load (bottom). | 201 |
| Figure 8.8 - Magnitude of the 5 th , 13 th , 15 th , and 17 th harmonics of the fundamental frequency using the OTFT technique as a function of load. | 203 |
| Figure 8.9 - Magnitude of the 19 th , 35 th , and 37 th harmonics of the fundamental frequency using the OTFT technique as a function of load. | 204 |
| Figure 8.10 - Wavelet plots of the induced rundown voltage on the healthy motor (top) and the faulty motors with 4 BRB (bottom) running at no load. | 206 |
| Figure 8.11 - Wavelet plots of the induced rundown voltage on the healthy motor (top) and faulty motors with 4 BRB (bottom) running at rated load. | 206 |
| Figure 8.12 – Change in wavelet scale, Δa , of the rundown induced voltage over a given time interval. | 208 |
| Figure 8.13 - Rundown stator magnetic flux linkage on the healthy motor when operating at no-load (top) and full-load (bottom) before and after the supply disconnection (at 0 s). | 210 |
| Figure 8.14 - Rundown stator magnetic flux linkage on the faulty motor with 4 BRB when operating at no-load (top) and full-load (bottom) before and after the supply disconnection (at 0 s). | 210 |
| Figure 8.15 – Step change in the stator magnetic flux linkage at the instant of supply disconnection under different loading conditions. | 212 |
| Figure 8.16 - Locus of the space vector of the stator flux-linkage for the healthy motor running at full load. | 213 |

| | |
|--|-----|
| Figure 8.17 - Locus of the space vector of the stator flux-linkage for the faulty motor with 4 BRB running at full load..... | 214 |
| Figure 8.18 – Flux linkage space vector magnitude of the healthy and faulty with 4BRB motors running at full load..... | 215 |
| Figure 8.19 - Time constant of the stator magnetic flux linkage after supply disconnection under different loading conditions. | 216 |
| Figure 8.20 - Harmonic spectra of the space vector magnitude of the healthy motor running at no load (top) and full load (bottom) using the standard FT. | 218 |
| Figure 8.21 - Harmonic spectra of the space vector magnitude of the faulty motor with 4 BRB running at no load (top) and full load (bottom) using the standard FT..... | 219 |
| Figure 8.22 - Harmonic spectra of the space vector magnitude of the healthy motor as in Figure 8.20 using the spatial FT. | 219 |
| Figure 8.23 - Harmonic spectra of the space vector magnitude of the faulty motor with 4 BRB as in Figure 8.21 using the spatial FT. | 220 |
| Figure 8.24 - Magnitude of the 18 th harmonic from the standard FT under different loading conditions. | 221 |
| Figure 8.25 - Magnitude of the 18 th harmonic from the spatial FT under different loading conditions. | 222 |

Symbols

| | |
|-----------|---|
| a | wavelet scale |
| a_{brb} | amplitudes of the BRB component |
| a_f | amplitudes of the fundamental signal component |
| c | number of coils of each stator phase |
| D_r | external rotor diameter |
| F | Fourier transform |
| f | supply frequency |
| f_{brb} | broken rotor bar sidebands |
| f_{de} | dynamic eccentricity fault frequency component |
| f_{de} | dynamic eccentricity fault frequency components |
| f_r | frequency corresponding to the rotor mechanical speed |
| f_{rsp} | rotor slot passing frequency |
| f_s | sampling frequency |

| | |
|---------------|--|
| f_{se} | static eccentricity fault frequency components |
| f_{sede} | static and dynamic eccentricity fault frequency components |
| f_{st} | shorted turn fault frequency components |
| ft | feature |
| $i(t)$ | steady-state stator current |
| i_{brb} | BRB component |
| i_f | fundamental signal component |
| $i_{rb}(t)$ | rotor bar current |
| $I_{rv\ max}$ | maximum value of the v th harmonic rotor current |
| I_s | maximum value of the stator phase current |
| $i_s(t)$ | steady-state signal components |
| $i_{sI}(t)$ | steady-state BRB sideband modulated at the fundamental frequency |
| $i_{so}(t)$ | other steady-state signal components that make up the stator current |
| $i_{sw}(t)$ | stator winding current |
| k | real integers |
| k_s, k_r | factors associated with the leakage inductance in the stator windings and the rotor cage |
| l | loading conditions |
| l_c | core length |
| N | number of samples |
| $n(t)$ | noise components |
| n_d | eccentricity constant |
| N_{ft} | number of features selected for a load |
| N_s | number of turns of each stator coil |
| n_s | synchronous speed |

| | |
|--------------------------------------|--|
| p | number of pole pairs |
| R | number of rotor bars/meshes |
| \mathbf{S} | power spectrum |
| s | per unit slip |
| t | time variable |
| t_s | sampling frequency |
| $V_{a(rms)}, V_{b(rms)}, V_{c(rms)}$ | RMS values of the three phase voltages of the motor |
| \mathbf{W} | wavelet transform |
| w | weight of a feature |
| x | circumferential angular position |
| x_1, x_2 | defined angular positions of the α^{th} mesh |
| α | real integers |
| β | real integers |
| δ | air gap length |
| $\varepsilon(t)$ | induced back emf |
| $\lambda(t)$ | stator magnetic flux linkage |
| μ_o | magnetic permeability of air |
| ν | order of the stator time harmonics |
| ν_s | stator MMF space harmonic rank |
| τ_{cb} | b^{th} coil pitch |
| τ_{cr} | rotor equivalent coil pitch |
| τ_p | pole step |
| φ | wavelet position |
| $\psi(t)$ | wavelet function |
| ω | angular frequency |

| | |
|------------|--------------------------|
| ω_r | angular rotor frequency |
| ω_s | angular supply frequency |

Abbreviations

| | |
|------|---------------------------------|
| A/D | analogue to digital |
| BRB | broken rotor bar |
| CU | current unbalance |
| CWT | continuous wavelet transform |
| DE | dynamic eccentricity |
| DEH | driving end horizontal |
| DEV | driving end vertical |
| DFT | discrete Fourier transform |
| DOL | direct-on-line |
| DWT | discrete wavelet transform |
| EPVA | extended Park's vector approach |
| FFT | fast Fourier transform |
| FT | Fourier transform |

| | |
|-------|---------------------------------------|
| MRF | multiple reference frame |
| MUSIC | multiple signal classification |
| NDEH | non-driving end horizontal |
| OTFT | order tracking Fourier transform |
| PSH | principal slot harmonics |
| s.d. | standard deviation |
| SE | static eccentricity |
| SNR | signal to noise ratio |
| STDFT | short time discrete Fourier transform |
| STFT | short-time Fourier transform |
| UF | unbalanced factor |
| UMP | unbalanced magnetic pull |
| WFA | winding function approach |
| WLC | weighted linear combination |
| WT | wavelet transform |